17

Hubbard, S. M., B. W. Romans, and S. A. Graham, 2007, An outcrop example of large-scale conglomeratic intrusions sourced from deep-water channel deposits, Cerro Toro Formation, Magallanes basin, southern Chile, *in* A. Hurst and J. Cartwright, eds., Sand injectites: Implications for hydrocarbon exploration and production: AAPG Memoir 87, p. 199–207.

An Outcrop Example of Large-scale Conglomeratic Intrusions Sourced from Deep-water Channel Deposits, Cerro Toro Formation, Magallanes Basin, Southern Chile

Stephen M. Hubbard

Department of Geological and Environmental Sciences, Stanford University, Stanford, California, U.S.A.

Stephan A. Graham

Department of Geological and Environmental Sciences, Stanford University, Stanford, California, U.S.A.

Brian W. Romans

Department of Geological and Environmental Sciences, Stanford University, Stanford, California, U.S.A.

ABSTRACT

Large-scale vertical to subvertical clastic intrusions (as much as 67 m [219 ft] wide and >100 m [>330 ft] high) are present in Cretaceous strata (Cerro Toro Formation) of the Ultima Esperanza district, southern Chile. The injectites emanate from the margins of submarine-channel deposits that accumulated at water depths of 1000–2000 m (3300–6600 ft) in the Magallanes foreland basin. The remobilized sediment is very coarse, consisting of sandy matrix conglomerate, muddy matrix conglomerate, and poorly sorted sandstone. The injectite bodies sometimes bifurcate upward and are circular in plan view and, thus, are geometrically analogous in many respects to numerous injection features mapped seismically in the North Sea Basin.

The remobilization of coarse sediment was likely induced after the burial of the parent deposit to at least a few hundred meters. The controlling factors on injection are difficult to discern; however, it is probable that the highly energetic process involved gas charging of the source body and, potentially, a seismic event trigger associated with the uplift of the Patagonian Andes.

DOI:10.1306/1209863M873265

INTRODUCTION

Clastic intrusions have been described and interpreted for more than 100 yr (e.g., Murchison, 1827; Diller, 1889; Newsom, 1903). A recent resurgence in the analysis and interpretation of sandstone dikes and sills in deep-water strata has been triggered largely by the pervasive occurrence of such features in petroliferous Paleogene deposits of the North Sea Basin (e.g., Duranti et al., 2002; Molyneux et al., 2002; Huuse et al., 2003; Huuse and Mickelson, 2004). Significant post-depositional remobilization of clastic material through injection processes adds complexity to both facies distribution and reservoir architecture. Recent advances in three-dimensional (3-D) seismic technology have made recognition and interpretation of associated features in the subsurface possible (e.g., MacLeod et al., 1999; Huuse and Mickelson, 2004; Huuse et al., 2004); however, characterization of the lithofacies associated with these large-scale injection features is limited to a few outcrop (e.g., Thompson et al., 1999; Surlyk and Noe-Nygaard, 2001) and drill-core data sets (e.g., Dixon et al., 1995; Hillier and Cosgrove, 2002; Purvis et al., 2002; Duranti and Hurst, 2004).

A Cretaceous clastic dike field that crops out in the Magallanes basin of southern Chile represents an excellent analog to some of the intrusive bodies in the North Sea Basin. The objectives of this chapter are to (1) describe and interpret the associated lithofacies of the intrusions, (2) document geometric relationships between the large-scale injectites and their source deposits, and (3) discuss the utility of these features as reservoir analogs.

STUDY AREA AND BACKGROUND GEOLOGY

During the Late Cretaceous, deep-water sediments of the Cerro Toro Formation accumulated in the Magallanes foreland basin of southern Chile. The elongate basin was characterized by a north–south-trending foredeep adjacent to the rising Andean Cordillera to the west. Based on paleocurrent data indicating north-to-south transport, Winn and Dott (1979) envisioned a southward-prograding deep-sea fan system fed from a canyon to the north into an extensive, basin-axial channel belt that was present for more than 100 km (62 mi) from the north of the Torres del Paine to the south of Puerto Natales (Figure 1). Lateral conduits into the southward-flowing fan-channel complex sourced directly from the Andean Cordillera to the west are postulated to have also contributed significant sediment into the basin (Crane and Lowe, 2001; Sohn et al., 2002).

The Cerro Toro Formation has proved to be of great interest to sedimentologists and petroleum geologists throughout the last few decades. Conglomeratic gravity-flow deposits including dunes 4 m (13 ft) in height, as well as gravelly plane lamination present in outcrops of the formation, have improved our general understanding of deep-water sedimentation mechanics (Winn and Dott, 1977; Sohn et al., 2002). Interpretations of deep-water channel processes have been made based on exceptional exposures of channel-overbank facies transitions in associated outcrops (Winn and Dott, 1979; Beaubouef, 2004; Crane, 2004; Hubbard et al., 2004). These same outcrops are considered to be geometrically excellent analogs to hydrocarbon reservoirs from across the globe (e.g., DeVries and Lindholm, 1994; Coleman, 2000; Beaubouef, 2004).

The area of interest in this study is located approximately 20 km (12 mi) north of the town of Puerto Natales in southern Chile, along the southern shore of Lago Sofia (Figure 1). The Cerro Toro Formation in this region can be divided into numerous distinctive intervals present over a stratigraphic thickness of approximately 2000–2500 m (6600–8200 ft) (Figure 2). Hundreds of meters of thin-bedded turbiditic shale and sandstone characterize the lowermost division of the formation, deposited during a period of relative quiescence in the Magallanes basin foredeep. A laterally discontinuous conglomerate body 75 m (246 ft) thick sharply overlies the fine-grained interval, suggesting a drastic change in sediment source area and delivery of coarse detritus into the basin. After a pause in coarse-grained sedimentation (recorded by the accumulation of ~150 m [~492 ft] of thin- to thick-bedded turbidite beds), more than 500 m (1640 ft) of conglomeratic beds accumulated across the basin foredeep. As flow into the basin waned overall, 300 m (984 ft) of gravity-flow deposits accumulated, ranging from thin-bedded turbidites, erosive sandy high-density turbidity-current deposits, and conglomeratic units with dunes 4 m (13 ft) high. The formation is capped by a thick package (hundreds of meters) of fine-grained bathyal deposits.

SEDIMENTARY FACIES

The strata of interest in this study include the lowermost conglomeratic interval of the Cerro Toro Formation and the overlying thin-bedded turbiditic units (beneath the 500-m [1640-ft]-thick conglomeratic interval; Figure 2). A detailed measured section through this interval is presented in Figure 3. The lithofacies recognized within this interval include concordant, bed-parallel deposits, as well as discordant chaotic deposits (nonparallel to bedding). Following the terminology used by Duranti and Hurst (2004), the bed-parallel deposits are referred to as stratified facies, and those deposits discordant with bedding orientation are considered unstratified facies. The lithofacies identified within the interval studied include (1) stratified thin-bedded sandstone and mudstone, (2) stratified thick-bedded sandstone, (3) stratified conglomerate, (4) unstratified conglomerate, and (5) unstratified poorly sorted sandstone.

Lithofacies 1: Stratified Thin-bedded Sandstone and Mudstone

Description

Stratified thin-bedded sandstone and mudstone constitute lithofacies 1 (L1). Individual sandstone beds range from less than 5 to 40 cm (2–15 in.) in thickness and are generally tabular for hundreds of meters. They are composed of fine- to lower medium-grained sandstone, normally graded and characterized by partial (T_{b-c} divisions typically) Bouma sequences. Soft-sediment deformation is present locally within sandstone beds (Figure 4). Mudstone interbeds are considered to be genetically linked to sandstone beds.

Sedimentation units of L1 are present lateral to, overlying, and underlying packages of conglomeratic material of lithofacies 3 (L3). They are observed to bend beneath overlying conglomeratic bodies and are upturned where they abut against vertical exposures of lithofacies 4 (L4) (Figure 4).

Interpretation

L1 represents the deposits of waning, low-density turbidity currents and are similar to facies interpreted as distal fan or out-of-channel deposits in numerous studies (e.g., Mutti and Ricci Lucchi, 1972; Walker, 1978; Mutti and Normark, 1991). Structural deformation of beds resulted from the differential compaction of conglomeratic and fine-grained units.

Lithofacies 2: Stratified Thick-bedded Sandstone

Description

Lithofacies 2 (L2) comprises thick-bedded sandstone. Beds are 0.5–2 m (1.6–6.6 ft) thick and, in places, are separated by thin, mudstone beds. They are tabular to slightly lenticular laterally and commonly fine upward from lower coarse- to medium-grained sandstone. Most beds associated with this lithofacies are structureless, although near-complete Bouma sequences are preserved locally (Figure 5). Inversely graded intervals (3–5 cm [1.2–2 in.] thick) are notable at the bases of some structureless units (Figure 5). Sharp, erosive bases are characteristic, uncommonly associated with mudstone rip-up clasts 1–2 cm (0.4–0.8 in.) in diameter.

Stratigraphically, sedimentation units of L2 are observed to increase in regularity at the top of the detailed measured section, prior to the onset of conglomeratic deposition (Figure 3).

Interpretation

The thick-bedded sandstone units of L2 record deposition from low-density (traction structured beds) or erosive high-density (structureless) turbidity currents. Normally graded, structureless beds are interpreted as S_3 divisions of Lowe, (1982); inversely graded bases of units are indicative of traction carpet deposition (S_1 divisions of Lowe, 1982). This lithofacies is transitional, recording gravity-flow energy intermediate between those flows, which deposited L1 (smaller, low-density flows) and L3 (conglomeratic flows).

Lithofacies 3: Stratified Conglomerate

Description

Lithofacies 3 (L3) consists of stratified conglomerate. Individual beds are greater than 4 m (13 ft) in thickness with sharp bases. Bed contacts are commonly difficult to discern because of textural homogeneity in this lithofacies; therefore, individual sedimentation units (deposits of an individual gravity-flow event) are difficult to correlate. Clasts are 3–5 cm (1.2–2 in.) in diameter on average, as much as 31 cm (12.2 in.) maximum, and are weakly imbricated in places (flow direction south-southwest, consistent with measurements made by Scott, 1966; Winn and Dott, 1979). Units are typically clast supported, and the matrix is texturally variable, consisting of well-sorted medium-grained sandstone, poorly sorted silty sandstone, or silty mudstone. Angular blocks of sandstone or mudstone 20–200 cm (7.8–78 in.) in diameter are uncommon to moderately abundant in associated units, normally in a state of partial disaggregation (Figure 6). Individual units are observed to be massive or normally graded. Scour surfaces with 1–3-m (3.3–9.8-ft) relief and subtle large-scale cross-stratification are present locally. In one instance, a scour 12 m (39 ft) deep and at least 60 m (196 ft) wide is filled with thin-bedded sandstone and mudstone (L1) (Figure 7).

Multiple sedimentation units associated with L3 comprise composite conglomerate bodies that are in sharp lateral contact with thin-bedded units of L1 (Figure 7). The margins of these composite sedimentary bodies are closely related to overlying, texturally similar features characterized by deposits of L4.

Interpretation

Lithofacies 3 is interpreted as sediment gravity-flow deposits. Sedimentation units that are structureless and normally graded are interpreted as the deposits of high-density turbidity currents (R_3 beds of Lowe, 1982). Large-scale cross-stratification records traction processes driven by turbulent flow. Deep and broad scours are also indicative of highly turbulent, channelized flow. Sediment blocks in the lithofacies represent rip-up clasts or raft blocks; localized occurrences of muddy matrix is related to the disaggregation of these sediment blocks.

Sedimentary features, including consistent paleocurrent measurements and the laterally lenticular shape of the composite conglomerate body, suggest that L3 was deposited within a submarine-channel complex.

Lithofacies 4: Unstratified Conglomerate

Description

Lithofacies 4 (L4) is composed of matrix- to clast-supported conglomerate (Figure 8A, C). Sediment bodies range in measurable thickness from 2 to 67 m (6.6 to 219 ft) in width and as much as approximately 130 m (426 ft) high (when combined with associated deposits of lithofacies 5 [L5]), sharply crosscutting bedded fine-grained sediments of L1 (Figure 9). Because of outcrop constraints, it is possible that the maximum width of the sedimentary bodies is greater than that which is recordable in the field. Subtle vertical alignment and sorting of grains is apparent locally, defining features that parallel the vertical margins of the conglomeratic bodies. The largest sedimentary body composed of L4 is clast supported at the core (maximum clast size is 8 cm [3.1 in.], and the average is 2–3 cm [0.8–1.18 in.]), and matrix to clast supported at the edges (maximum clast size is 14 cm [5.5 in.], and the average is 3–4 cm [1.1–1.5 in.]). In one locality, a thin (10-cm; 4-in.) sandstone layer is preserved at the edge of the conglomerate body parallel to its margin. This sandstone layer, as well as associated conglomerate, is characterized by nearly vertically oriented flute- or groovelike structures (Figure 8). Matrix material consists of poorly sorted sandstone and mudstone; notably, the matrix is more mud rich toward the margins of the sediment body in some instances. Large mudstone and sandstone blocks as much as 0.4 m (1.3 ft) in diameter are present within the deposits (Figure 8).

Lithofacies 4 is closely associated with the margins of underlying stratified conglomerate bodies (L3). It is observed to grade upward into deposits of L5.

Interpretation

The geometry of deposits of L4 unequivocally indicates that associated units were emplaced by postdepositional remobilization processes. The deposits of L4 represent large-scale injectites that were sourced from the margins of underlying channel deposits of L3. Discordant contacts between the host strata of L1 and the injected material of L4 are consistent with the interpretation that the bodies were emplaced in a fluidized state (Surlyk and Noe-Nygaard, 2001; Duranti and Hurst, 2004). Textural gradation from the middle of the bodies to the margins also supports this interpretation. Vertical stratification parallel to the walls of the injectite is perhaps the conglomeratic expression of similarly oriented flow structures in sandstone dikes (Peterson, 1968). The process of fluid escape and sediment transport upward through the dike may have been maintained by an impermeable barrier of muddy matrix-supported conglomerate toward the edges of the sediment body, which served to confine the flow (cf. Lowe, 1975; Mount, 1993). Sedimentary rip-up clasts were locally derived from the host strata. Elongate, flutelike features record the orientation of injectite expulsion, inferred to have been upward from the margin of the channel deposits of L3. Rip-up material and flutelike grooves suggest that the flow of injected material was supported by turbulence in a manner similar to gravity flows, with the exception that the injected material was driven by overpressure in the source deposit instead of gravity.

Lithofacies 5: Unstratified Poorly Sorted Sandstone

Description

Lithofacies 5 consists of poorly sorted sandstone (medium-grained average) with interdispersed pebbles. Deposits grade upward and away from the conglomeratic L4 (Figure 10), and as part of the same sediment bodies, they share the same crosscutting relationships with the surrounding strata.

Interpretation

Sandy deposits of L5 are intrusive, genetically linked to the conglomeratic deposits (L4) from which they grade. The normally graded nature of the intrusive bodies (from the conglomeratic L4 to the sandstone of L5) results from the reduced competence of the remobilized sandstone and conglomerate mixture as it was forced upward through the stratigraphic column.

Lithofacies Distribution

The injectites at Lago Sofia were first reported by Robert Dott and his students in the 1960s and 1970s (Scott, 1966; Winn and Dott, 1979). Schmitt (1991) mapped and described the 3-D exposure of features in detail. We present our geological mapping of lithofacies distribution in the study area in Figure 11. An oblique aerial photograph and line-drawing trace of the dominant features are presented in Figure 12.

Three distinctive conglomeratic channel bodies (L3) are present in the study area (C1–C3; Figures 11, 12). Four injectite bodies are observed, emanating upward from the channel deposits (I1–I4; Figures 11, 12). The westernmost depositional element (C1) is the largest and stratigraphically lowest, with size of the composite channel bodies decreasing progressively eastward (Figure 7). Margins of channel body C1 are steep; the upper part of the eastern margin is characterized by a broad wing, similar to features known to have resulted from the injection of remobilized sediment in other deep-water deposits (cf. Dixon et al., 1995; Lonergan et al., 2000; Duranti et al., 2002). The flutelike grooves present at the top of the western margin are interpreted to have been generated through the injection of coarse material upward into the thin-bedded, muddy turbidites (L1). The injectite body (I1) is the widest observed in the study area, at almost 70 m (229 ft) in width. The stratigraphic thickness of I1 is not discernable because of Holocene glacial erosion that has removed a significant thickness of strata. The eastern margin of channel body C1 is associated with a discontinuously exposed intrusive body (I2) (Figure 11). I1 and I2 nearly intersect to form a circular composite body. Circular (in plan view) or conical intrusions have been extensively documented from the subsurface in the North Sea Basin (Molyneux et al., 2002; Hurst et al., 2003b; Huuse and Mickelson, 2004).

Channel body C2 is associated with a bifurcating intrusion (I3) that extends upward approximately 130 m (426 ft) from its western margin (Figures 11, 12), with a maximum width of 22 m (72 ft). The western bifurcation of I3 is characterized by vertical grain-size segregation. Unstratified conglomerate (L4) grades upward into the unstratified sandstone (L5), as mapped in Figure 11. The eastern bifurcation of I3 is draped by thin-bedded turbidites that have been structurally curved around the head of the injectite body as a result of differential compaction upon burial (Figure 9C). In 3-D, it is possible that this bifurcation represents the edges of an intrusion that was conical (cf. Molyneux et al., 2002; Hurst et al., 2003b). Notably, at two stratigraphic horizons (near the middle and at the very top of the vertically exposed injectite), conglomeratic material is observed to have been diverted off the vertical injection path, following a bedding plane for as much as 10 m (33 ft) (Figure 13A). The easternmost channel body (C3) is the smallest, associated with a relatively diminutive (2.5-m [8.2-ft]-wide and 45-m [147-ft]-high) vertical intrusion (Figures 11, 12).

The intrusions mapped in the Cerro Toro Formation strike in various directions, defining an overall polygonal arrangement (Figure 14). Controls on this pattern of injections are difficult to discern from the outcrop data. Cartwright (1994) and Lonergan and Cartwright (1999) documented a polygonal fault-dominated terrane in Eocene strata of the North Sea; these faults have been postulated to at least partially control the distribution of sandstone intrusions (Molyneux et al., 2002; Huuse et al., 2003). Faults with orientations consistent with the intrusions have not yet been recognized in the Cerro Toro Formation. Such faults, if present, may be masked in fine-grained sediments that are commonly covered by vegetation in the study area. Further fieldwork is needed to assess the presence or absence of structures that may have controlled intrusion geometry. Clastic intrusions intimately related to faulting in younger deep-water strata of the Magallanes basin have been documented (Shultz and Hubbard, 2005).

INTRUSION EMPLACEMENT

The process of remobilizing sediment in the subsurface is understood to involve (1) an unconsolidated parent sediment body, (2) overpressure development in the parent sediment body, (3) failure of the top seal of the overpressured parental sediment body, and (4) vertical pressure gradient driving upward flow of the injection material. Fine sand has been theoretically proven to be the most efficient grain size to be fluidized (Richardson, 1971), and consequently, most of the intrusions documented from the geologic record are composed of fine-grained sandstone. However, coarsely granular intrusive material (Archer, 1984), as well as injected sandstone with meter-scale sediment blocks, has been documented (Huuse et al., 2005). The conglomeratic material in the Cerro Toro Formation apparently represents the coarsest intrusive deposits documented from the geologic record. Jolly and Lonergan (2002) suggested that coarse injectite material reflects extremely high injection velocities, although the mechanism of remobilizing gravelly sediment in the subsurface is not well understood.

Small-scale injectites are most likely to have formed close to the sediment-water interface, commonly triggered by deposition of overlying sediment (e.g., Hiscott, 1979; Archer, 1984). Conversely, larger vertical features like those observed in the Cerro Toro Formation are likely associated with relatively deep burial of at least a few hundred meters (Jolly and Lonergan, 2002;

Hurst et al., 2003a). Schmitt (1991) suggested that the intrusions in the Cerro Toro Formation originated in response to the structural development of the Andean Cordillera. She recognized, however, that liquefaction of conglomeratic material is not easily accomplished, especially through earthquake-induced shaking alone. A scenario where extremely high pore-fluid pressures developed in the source sediment body associated with a high concentration of methane was favored (Schmitt, 1991). Fluidization of sand bodies resulting from overpressure generated in response to an increase in methane concentration has been interpreted for injectites in other basins (Jenkins, 1930; Brooke et al., 1995; Nichols, 1995). Unraveling the geological history of the deposits studied in the Cerro Toro Formation represents a topic of continued research; however, based on field observations and published work on other large-scale injectites in the North Sea Basin, it is speculated to have involved (1) deposition of deep-water conglomeratic sediment in a submarine channel complex, later sealed by deposition of fine-grained sediments; (2) pore-pressure buildup in the unconsolidated depositional body through gas charging; (3) a trigger, such as a seismic event related to the uplifting Andes, causing fluidization of the sediment; and (4) rupture of the fine-grained seal at the margins of the depositional bodies, creating a situation conducive for the upward intrusion of conglomeratic sediment.

The minimum fluidization velocity for injected sands and small mudstone clasts was calculated to be in the order of as much as 0.1–0.5 m s^{-1} (0.3–1.6 ft s^{-1}) by Duranti and Hurst (2004), although they calculated values as much as 10 m s^{-1} (33 ft s^{-1}) for some intrusive events. Using the square-root law outlined in Allen (1985), a minimum fluidization velocity for the injected gravel at Lago Sofia (maximum clast size used = 20 cm [8 in.]) is calculated to be approximately 70 cm s^{-1} (see appendix 1 of Duranti and Hurst, 2004, for more information on the calculation). This is well above the value where flow in a dike becomes turbulent (<5 cm s^{-1} [<2 in. s^{-1}] according to Schmitt, 1991). The normally graded character of intrusion I3 indicates that turbulence was an important process in the remobilization of sediment in the study area (Schmitt, 1991).

IMPLICATIONS FOR HYDROCARBON EXPLORATION AND DEVELOPMENT

The capability of clastic dikes and sills to act as conduits for fluids in the subsurface is well understood (Jenkins, 1930; Thompson et al., 1999; Hurst et al., 2003b). Lonergan et al. (2000) recognized that sediment remobilization has the potential to affect reservoir architecture, reservoir properties through the homogenization of texture, and communicability between reservoir bodies, all of which influence reservoir volumetrics. The productivity of a particular unit can be affected either positively or negatively. In the Alba field of the North Sea, remobilized deposits have been drilled with excellent results (MacLeod et al., 1999); recognizing complicated reservoir geometry resulting from the presence of injectites has influenced both exploration (de Boer et al., 2007) and production strategies (Purvis et al., 2002). In other examples, it is possible that increased connectivity could result in a poor estimation of the location of the oil-water contact, resulting in a wet well (Lonergan et al., 2000). The intrusions in the Cerro Toro Formation occur within a succession of fine-grained turbiditic deposits, stratigraphically between two large, depositional sedimentary bodies. With the limited exposure of the outcrop, it is impossible to discern whether the intrusive material is connected to the two depositional units. Given a similar situation in the subsurface, connection of the large intrusive and depositional sediment bodies would completely change reservoir geometry and volumetrics and significantly change the optimal hydrocarbon development strategy.

Intrusion geometries similar to those observed in the Cerro Toro Formation have been documented in numerous publications. In particular, circular or conical features are common (Molyneux et al., 2002; Hurst et al., 2003b; Loseth et al., 2003; Huuse and Mickelson, 2004; Huuse et al., 2004), as are intrusions that emanate from the margins of channel deposits resulting in winglike geometries (e.g., Dixon et al., 1995; MacLeod et al., 1999; Duranti et al., 2002). A summary diagram comparing the intrusive bodies documented from outcrops of the Cerro Toro Formation with similar features imaged from the subsurface is presented in Figure 13.

Sediment remobilization had a significant effect on the texture and, subsequently, the petrophysical properties, of the Cerro Toro Formation. The large grain-clast sizes of the deposits serve to exemplify these effects. In the case where the depositional sediment body was characterized by poorly sorted and variable silty-sandstone to silty-mudstone matrix (injectite body I1), the associated injectite was observed to have lateral size segregation in matrix grain size in the vertical intrusion. The finer material was elutriated to the margins of the dike, whereas the higher reservoir-quality sandy material was concentrated in the center of the intrusive body. Where the depositional channel deposit consists of clast-supported conglomerate with a relatively well-sorted sandy matrix (channel body C2), a vertical segregation of grain size was observed, and conglomerate grades upward into sandstone. This grain-size distribution would have an important effect on fluid distribution and potential reservoir performance in a similar deposit in the subsurface; it is not certain whether similar, more subtle heterogeneities are present in some of the remobilized sandstone reservoirs in the North Sea. At the scale of an individual core, Duranti and Hurst (2004) noted that primary sedimentary structures were obliterated by intrusion processes, resulting in the common preservation of more massive deposits. Large pillars, distorted laminae, and mudstone breccias were also documented and interpreted to have resulted from fluid expulsion. Remobilized facies typically had reduced porosities and permeabilities resulting from the mixing of grain sizes. Because of the inherent limitations of core, large-scale grain-size trends (through an injectite tens to hundreds of meters in width and height) are not easily documented. Outcrops, such as that in the Cerro Toro Formation, represent the only way to observe these textural trends through an entire injectite sedimentary body. Furthermore, the 3-D nature of the exposure provides an opportunity to more accurately document and visualize the geometric configuration of the sediment bodies.

CONCLUSIONS

Outcropping sedimentary bodies in the Cerro Toro Formation of southern Chile represent an excellent opportunity to further our understanding of clastic intrusion processes and the properties of associated facies as they are preserved in the rock record. Sediment grain size associated with the deposits range from mud to cobbles, and as a result, numerous textural characteristics in the injectites are easily observed that provide insight into clastic intrusion mechanics. These include gradation from more muddy deposits at injectite walls to sandier material in the axes of intrusions and normal grading throughout the vertical length of injectite bodies. Despite the coarseness of sediment, evidence for turbulent-flow conditions during injection is present, including near vertically oriented flutelike structures and the presence of rip-up clasts in the injectite bodies. It is postulated that the violent injection process involved overpressure in the parent sedimentary bodies associated with gas charging and a possible tectonic triggering event related to the rise of the Andes.

Upward bifurcation and circular plan-view geometries are both observed in the study area, associated with the large-scale injections (as much as 67 m [219 ft] wide and >100 m [>330 ft] high). Geometrically, the Cerro Toro Formation injectites are arguably the best outcrop analogs found to date for numerous, economically important deposits of remobilized material common in deep-water clastic petroleum basins.

ACKNOWLEDGMENTS

We thank affiliate members of the Stanford Project on Deep-water Depositional Systems, including Anadarko, BP, ChevronTexaco, Emerald Trail LLC, Eni-Agip, ExxonMobil, Marathon, Nexen, Occidental, Petrobras, Rohöl-Aufsuchungs A.G., and Unocal for financial support of our research. Reviews by John Cosgrove, Adrian Hartley, and Andrew Hurst have improved the clarity of the manuscript and are greatly appreciated.

REFERENCES CITED

Allen, J. R. L., 1985, Principles of physical sedimentology: Boston, Allen and Unwin, 272 p.

Archer, J. B., 1984, Clastic intrusions in deep-sea fan deposits of the Rosroe Formation, Lower Ordovician, western Ireland: Journal of Sedimentary Petrology, v. 54, p. 1197–1205.

Beaubouef, R. T., 2004, Deep-water leveed-channel complexes of the Cerro Toro Formation, Upper Cretaceous, southern Chile: AAPG Bulletin, v. 88, p. 1471–1500.

Brooke, C. M., T. J. Trimble, and T. A. MacKay, 1995, Mounded shallow gas sands from the Quaternary of the North Sea: Analogues for the formation of sand mounds in deep water Tertiary sediments?, *in* A. J. Hartley and D. J. Prosser, eds., Characterization of deep marine clastic systems: Geological Society (London) Special Publication 94, p. 95–101.

Cartwright, J. A., 1994, Episodic basin-wide fluid expulsion from geopressured shale sequence in the North Sea Basin: Geology, v. 22, p. 447–450.

Coleman, J. L., 2000, Reassessment of the Cerro Toro (Chile) sandstones in view of channel-levee-overbank reservoir continuity issues, *in* P. Weimer, ed., Deep-water reservoirs of the world: Gulf Coast Section SEPM 20th Annual Research Conference, p. 252–258.

Crane, W. H., 2004, Depositional history of the Upper Cretaceous Cerro Toro Formation, Silo syncline, Magallanes basin, Chile: Ph.D. thesis, Stanford University, Stanford, California, 275 p.

Crane, W. H., and D. R. Lowe, 2001, Architecture of a Cretaceous channel-levee complex, Cerro Toro Formation, Magallanes basin, Chile (abs.): Geological Society of America Annual Meeting Abstracts with Programs, v. 33, p. 36.

de Boer, W., P. B. Rawlinson, and A. Hurst, 2007, Successful exploration of a sand injectite complex: Hamsun prospect, Norway Block 24/9, *in* A. Hurst and J. Cartwright, eds., Sand injectites: Implications for hydrocarbon exploration and production: AAPG Memoir 87, p. 65–68.

DeVries, M. B., and R. M. Lindholm, 1994, Internal architecture of a channel-levee complex, Cerro Toro Formation, southern Chile, *in* A. H. Bouma and B. G. Perkins, eds., Submarine fans and turbidite systems: Gulf Coast Section SEPM 15th Annual Research Conference, p. 105–114.

Diller, J. S., 1889, Sandstone dikes: Geological Society of America Bulletin, v. 1, p. 411–442.

Dixon, R. J., K. Schofield, R. Anderton, A. D. Reynolds, R. W. S. Alexander, M. C. Williams, and K. G. Davies, 1995, Sandstone diapirism and clastic intrusion in the Tertiary submarine fans of the Bruce-Beryl Embayment, Quadrant 9, UKCS, *in* A. J. Hartley and D. J. Prosser, eds., Characterization of deep marine clastic systems: Geological Society (London) Special Publication 94, p. 77–94.

Duranti, D., and A. Hurst, 2004, Fluidization and injection in the deep-water sandstones of the Eocene Alba Formation (UK North Sea): Sedimentology, v. 51, p. 1–27.

Duranti, D., A. Hurst, C. Bell, S. Groves, and R. Hanson, 2002, Injected and remobilized Eocene sandstones from the Alba field, UKCS: Core and wireline log characteristics: Petroleum Geoscience, v. 8, p. 99–107.

Fildani, A., T. D. Cope, S. A. Graham, and J. L. Wooden, 2003, Initiation of the Magallanes foreland basin: Timing of the southernmost Patagonian Andes orogeny revised by detrital zircon provenance analysis: Geology, v. 31, p. 1081–1084.

Hillier, R. D., and J. W. Cosgrove, 2002, Core and seismic observations of overpressure-related deformation within Eocene sediments of the outer Moray Firth, UKCS: Petroleum Geoscience, v. 8, p. 141–149.

Hiscott, R. N., 1979, Clastic sills and dikes associated with deep-water sandstones, Tourelle Formation, Ordovician, Quebec: Journal of Sedimentary Petrology, v. 49, p. 1–10.

Hubbard, S. M., B. R. Romans, S. A. Graham, and D. R. Lowe, 2004, Downstream variability in deep-water channel deposit character and associated sedimentary processes, Cretaceous Cerro Toro Formation outcrop belt, Magallanes basin, Chile 613 (abs.): Geological Society of America Annual Meeting Abstracts with Programs, v. 36, p. 373.

Hurst, A., J. Cartwright, and D. Duranti, 2003a, Fluidization structures produced by upward injection of sand through a sealing lithology, *in* P. Van Rensbergen, R. R. Hillis, A. J. Maltman, and C. K. Morley, eds., Subsurface sediment mobilization: Geological Society (London) Special Publication 216, p. 123–137.

Hurst, A., J. Cartwright, M. Huuse, R. Jonk, A. Schwab, D. Duranti, and B. Cronin, 2003b, Significance of large-scale sand injectites as long-term fluid conduits: Evidence from seismic data: Geofluids, v. 3, p. 263–274.

Huuse, M., and M. Mickelson, 2004, Eocene sandstone intrusions in the Tampen Spur area (Norwegian North Sea Quad 34) imaged by 3D seismic data: Marine and Petroleum Geology, v. 21, p. 141–155.

Huuse, M., D. Duranti, C. G. Guargena, P. Prat, K. Holm, N. Steinsland, B. T. Cronin, A. Hurst, and J. Cartwright, 2003, Sandstone intrusions: Detection and significance for exploration and production: First Break, v. 21, p. 15–24.

Huuse, M., D. Duranti, N. Steinsland, C. G. Guargena, P. Prat, K. Holm, J. Cartwright, and A. Hurst, 2004, Seismic characteristics of large-scale sandstone intrusions in the Paleogene of the south Viking Graben, UK and Norwegian North Sea, *in* R. J. Davies, J. A. Cartwright, S. A. Stewart, M. Lappin, and J. R. Underhill, eds., 3D seismic technology: Application to the exploration of sedimentary basins: Geological Society (London) Memoir 29, p. 263–277.

Huuse, M., S. J. Shoulders, D. I. Netoff, and J. Cartwright, 2005, Giant sandstone pipes record basin-scale liquefaction of buried dune sands in the Middle Jurassic of SE Utah: Terra Nova, v. 17, p. 593–596.

Jenkins, O. P., 1930, Sandstone dikes as conduits for oil migration through shales: AAPG Bulletin, v. 14, p. 411–421.

Jolly, R. J. H., and L. Lonergan, 2002, Mechanisms and controls on the formation of sand intrusions: Journal of the Geological Society (London), v. 159, p. 605–617.

Katz, H. R., 1963, Revision of Cretaceous stratigraphy in Patagonian cordillera of Ultima Esperanza, Magallanes Province, Chile: AAPG Bulletin, v. 47, p. 506–524.

Lonergan, L., and J. A. Cartwright, 1999, Polygonal faults and their influence on deep-water sandstone reservoir geometries, Alba field, United Kingdom central North Sea: AAPG Bulletin, v. 83, p. 410–432.

Lonergan, L., N. Lee, H. D. Johnson, J. A. Cartwright, and R. J. H. Jolly, 2000, Remobilization and injection in deepwater depositional systems: Implications for reservoir architecture and prediction, *in* P. Weimer, R. M. Slatt, J. Coleman, N. C. Rosen, H. Nelson, A. H. Bouma, M. J. Styzen, and D. T. Lawrence, eds., 13 deep-water reservoirs of the world: Gulf Coast Section SEPM Foundation 20th Annual Research Conference, p. 515–532.

Loseth, H., L. Wensaas, B. Arntsen, and M. Hovland, 2003, Gas and fluid injection triggering shallow mud mobilization in the Hordaland Group, North Sea, *in* P. Van Rensbergen, R. R. Hillis, A. J. Maltman, and C. K. Morley, eds., Subsurface sediment mobilization: Geological Society (London) Special Publication 216, p. 139–157.

Lowe, D. R., 1975, Water escape structures in coarse-grained sediments: Sedimentology, v. 22, p. 157–204.

Lowe, D. R., 1982, Sediment gravity flows: 2. Depositional models with special reference to the deposits of high-density turbidity currents: Journal of Sedimentary Petrology, v. 52, p. 279–297.

MacLeod, M. K., R. A. Hanson, C. R. Bell, and S. McHugo, 1999, The Alba field Ocean Bottom Cable Seismic survey: Impact on development: The Leading Edge, v. 18, p. 1306–1312.

Molyneux, S., J. Cartwright, and L. Lonergan, 2002, Conical sandstone injection structures imaged by 3D seismic in the central North Sea, UK: First Break, v. 20, p. 383–393.

Mount, J. F., 1993, Formation of fluidization pipes during liquefaction: Examples from the Uratanna Formation (Lower Cambrian), South Australia: Sedimentology, v. 40, p. 1027–1037.

Murchison, R. I., 1827, Supplementary remarks on the Oolitic Series in the counties of Sutherland and Ross, and in the Hebrides: Transactions of the Geological Society (London), v. 2, p. 353.

Mutti, E., and W. R. Normark, 1991, An integrated approach to the study of turbidite systems, *in* P. Weimer and H. Link, eds., Seismic facies and sedimentary processes of submarine fans and turbidite systems: New York, Springer-Verlag, p. 75–106.

Mutti, E., and F. Ricci Lucchi, 1972, Le torbiditi dell' Appennino settentrionale: Introduzione all'analisi di facies: Memorie della Societa Geologica Italiana, v. 11, p. 161–199.

Natland, M. L., P. E. Gonzalez, A. Canon, and M. Ernst, 1974, A system of stages for correlation of Magallanes basin sediments: AAPG Memoir 139, 126 p.

Newsom, J. F., 1903, Clastic dikes: Geological Society of America Bulletin, v. 14, p. 227–268.

Nichols, R. J., 1995, The liquification and remobilization of sandy sediments, *in* A. J. Hartley and D. J. Prosser, eds., Characterization of deep marine clastic systems: Geological Society (London) Special Publication 94, p. 63–76.

Peterson, G. L., 1968, Flow structures in sandstone dikes: Sedimentary Geology, v. 2, p. 177–190.

Purvis, K., J. Kao, K. Flanagan, J. Henderson, and D. Duranti, 2002, Complex reservoir geometries in a deep water clastic sequence, Gryphon field, UKCS: Injection structures, geological modeling and reservoir simulation: Marine and Petroleum Geology, v. 19, p. 161–179.

Richardson, J. F., 1971, Incipient fluidization and particulate systems, *in* J. F. Davidson and D. Harrison, eds., Fluidization: London, Academic Press, p. 25–64.

Schmitt, K. R., 1991, Sandstone intrusions in the Andean fold-thrust belt (51°–54° S): Implications for the paleohydrogeologic evolution of the southernmost Andes: Ph.D. thesis, Columbia University, New York, 263 p.

Scott, K. M., 1966, Sedimentology and dispersal pattern of a Cretaceous flysch sequence, Patagonian Andes, southern Chile: AAPG Bulletin, v. 50, p. 72–107.

Shultz, M. R., and S. M. Hubbard, 2005, Sedimentology, stratigraphic architecture, and ichnology of gravity-flow deposits partially ponded in a growth-fault-controlled slope minibasin, Tres Pasos Formation (Cretaceous), southern Chile: Journal of Sedimentary Research, v. 75, p. 443–456.

Sohn, Y. K., M. Y. Choe, and H. R. Jo, 2002, Transition from debris flow to hyperconcentrated flow in a submarine channel (the Cretaceous Cerro Toro Formation, southern Chile): Terra Nova, v. 14, p. 405–415.

Surlyk, F., and N. Noe-Nygaard, 2001, Sand remobilisation and intrusion in the Upper Jurassic Hareelv Formation of East Greenland: Bulletin of the Geological Society of Denmark, v. 48, p. 169–188.

Thompson, B. J., R. E. Garrison, and C. J. Moore, 1999, A late Cenozoic sandstone intrusion west of Santa Cruz, California: Fluidized flow of water and hydrocarbon-saturated sediments, *in* R. E. Garrison, I. W. Aiello, and J. C. Moore, eds., Late Cenozoic fluid seeps and tectonics along the San Gregorio fault zone in the Monterey Bay region, California: AAPG Pacific Section Volume and Guidebook GB-76, p. 53–74.

Walker, R. G., 1978, Deep-water sandstone facies and ancient submarine fans: Models for exploration for stratigraphic traps: AAPG Bulletin, v. 62, p. 932–966.

Wilson, T. J., 1991, Transition from back-arc to foreland basin development in the southernmost Andes: Stratigraphic record from the Ultima Espiranza district, Chile: Geological Society of America Bulletin, v. 103, p. 98–111.

Winn, R. D., and R. H. Dott Jr., 1977, Large-scale traction produced structures in deep-water fan-channel conglomerates in southern Chile: Geology, v. 5, p. 41–44.

Winn, R. D., and R. H. Dott Jr., 1979, Deep-water fan-channel conglomerates of the Late Cretaceous age, southern Chile: Sedimentology, v. 26, p. 203–228.

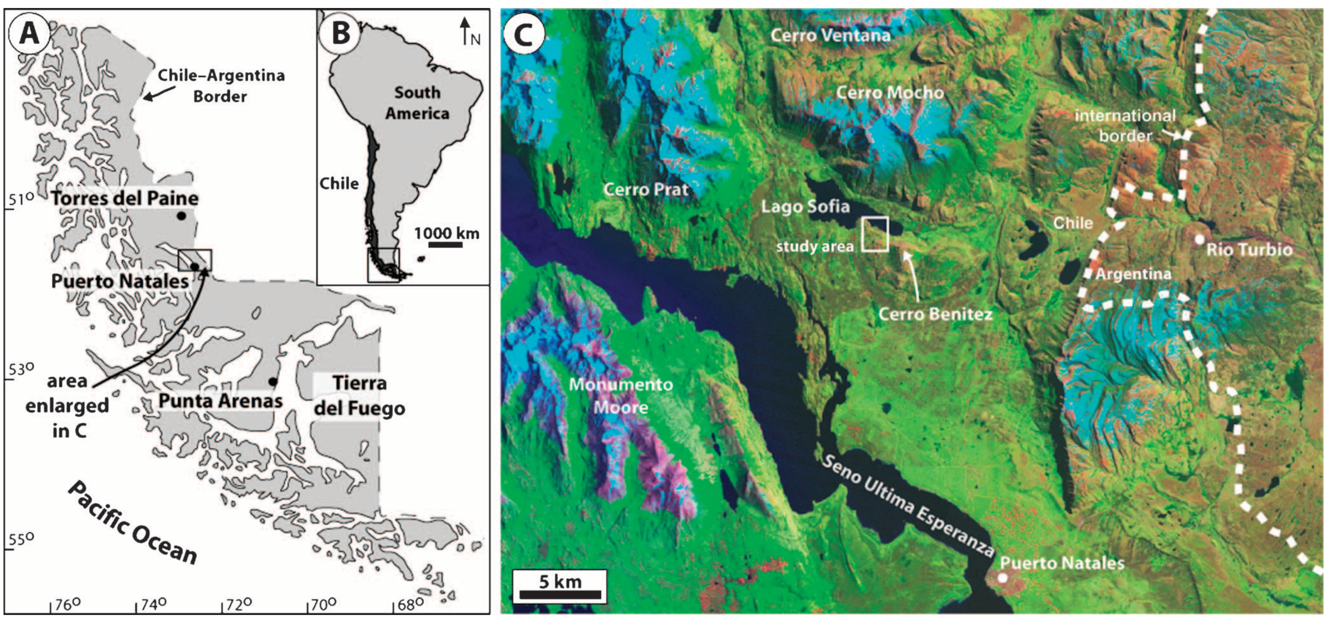

FIGURE 1. (A) Location of the study area in southernmost Chile. Inset of South America in (B). (C) Satellite image of the southern part of the Ultima Esperanza District highlighting the location of the outcrop focused on in this chapter, between the southern shore of Lago Sofia and the peak of Cerro Benitez.

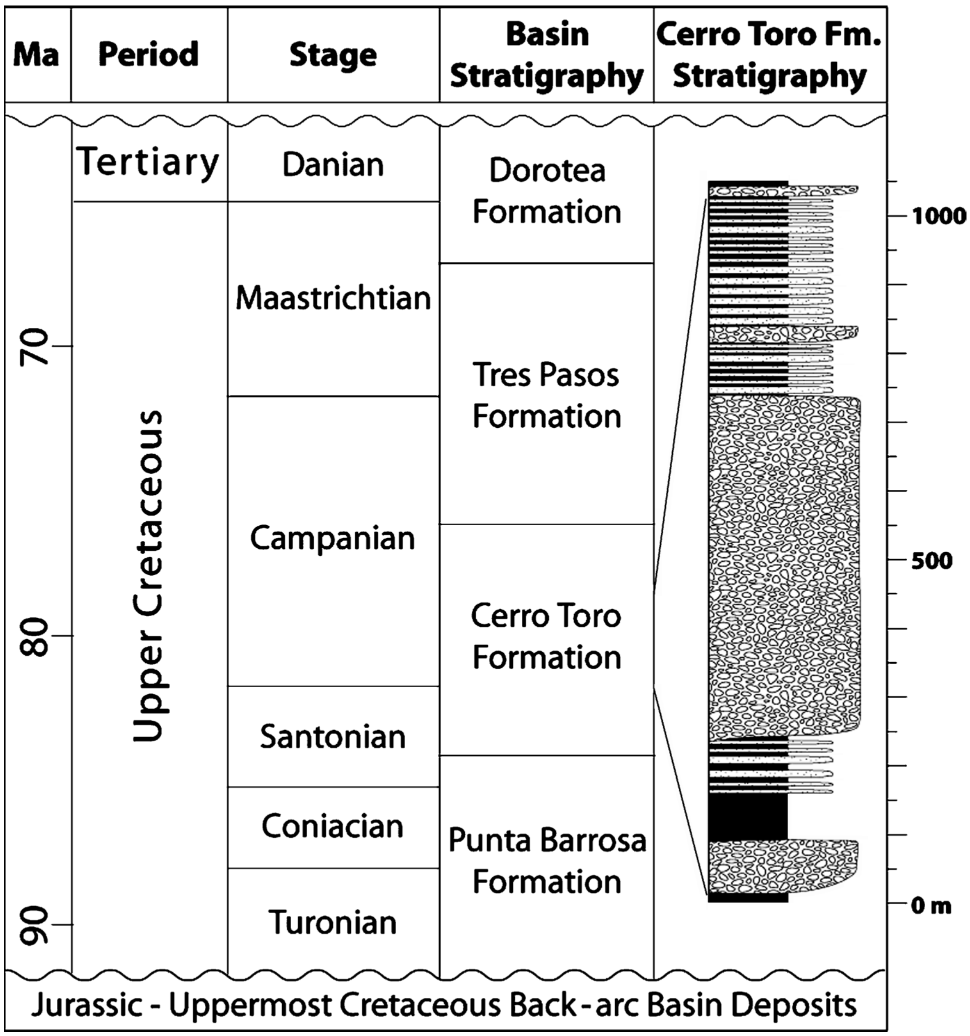

FIGURE 2. Upper Cretaceous stratigraphy of the Magallanes basin (compiled in part from Katz, 1963; Natland et al., 1974; Wilson, 1991; Fildani et al., 2003). The Cerro Toro Formation stratigraphy in the study area (based on a detail measured section) reveals that the conglomeratic interval is considerably thicker than previously reported by Scott (1966) and Winn and Dott (1979). Note that the scale at the right of the diagram only applies to the simplified measured section shown. The specific stratigraphic interval of interest in this study is between 0 and 300 m (0 and 984 ft).

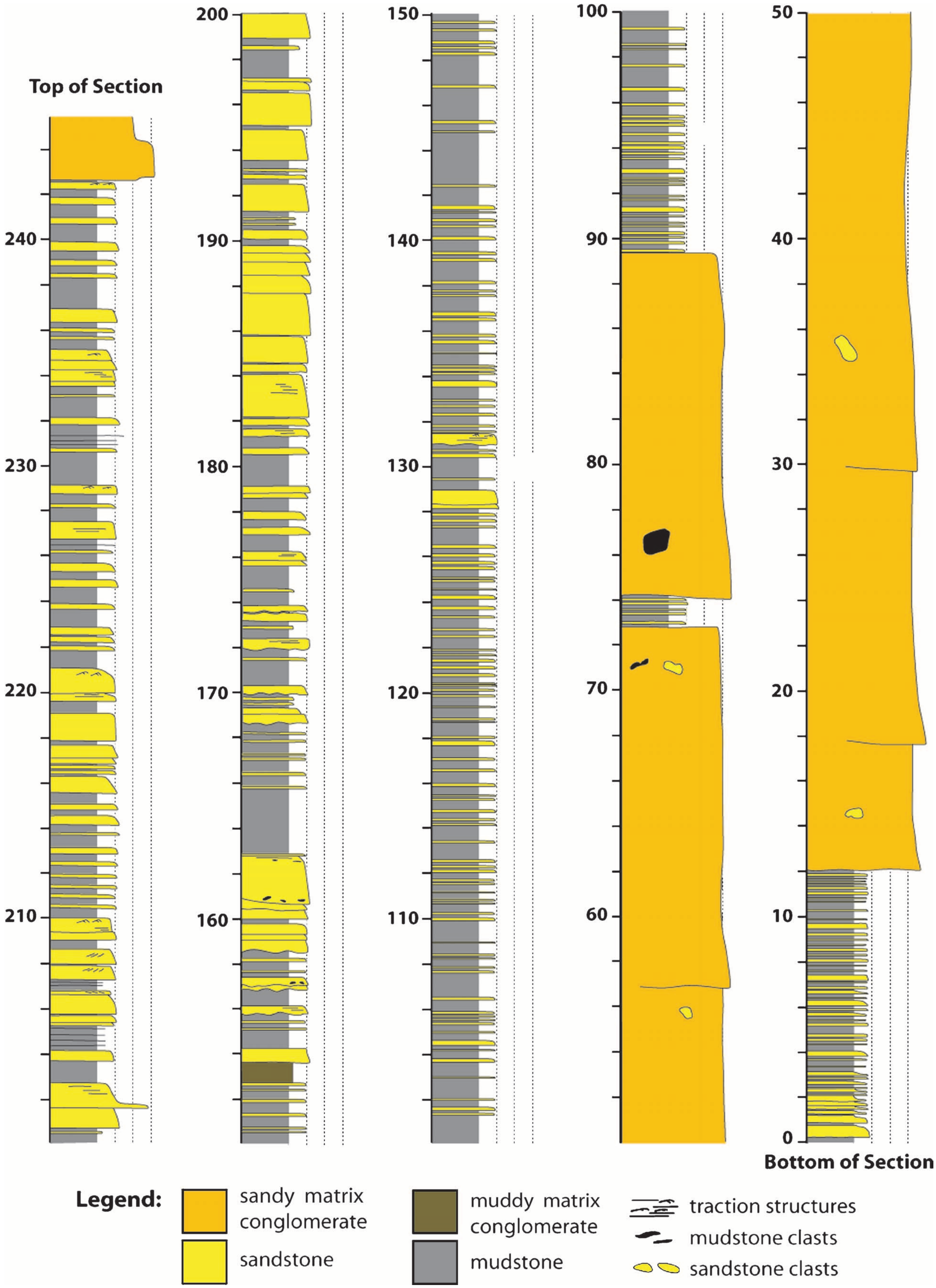

FIGURE 3. Measured section through the intruded stratigraphic interval studied in the lower part of the Cerro Toro Formation at Lago Sofia. Depth in meters.

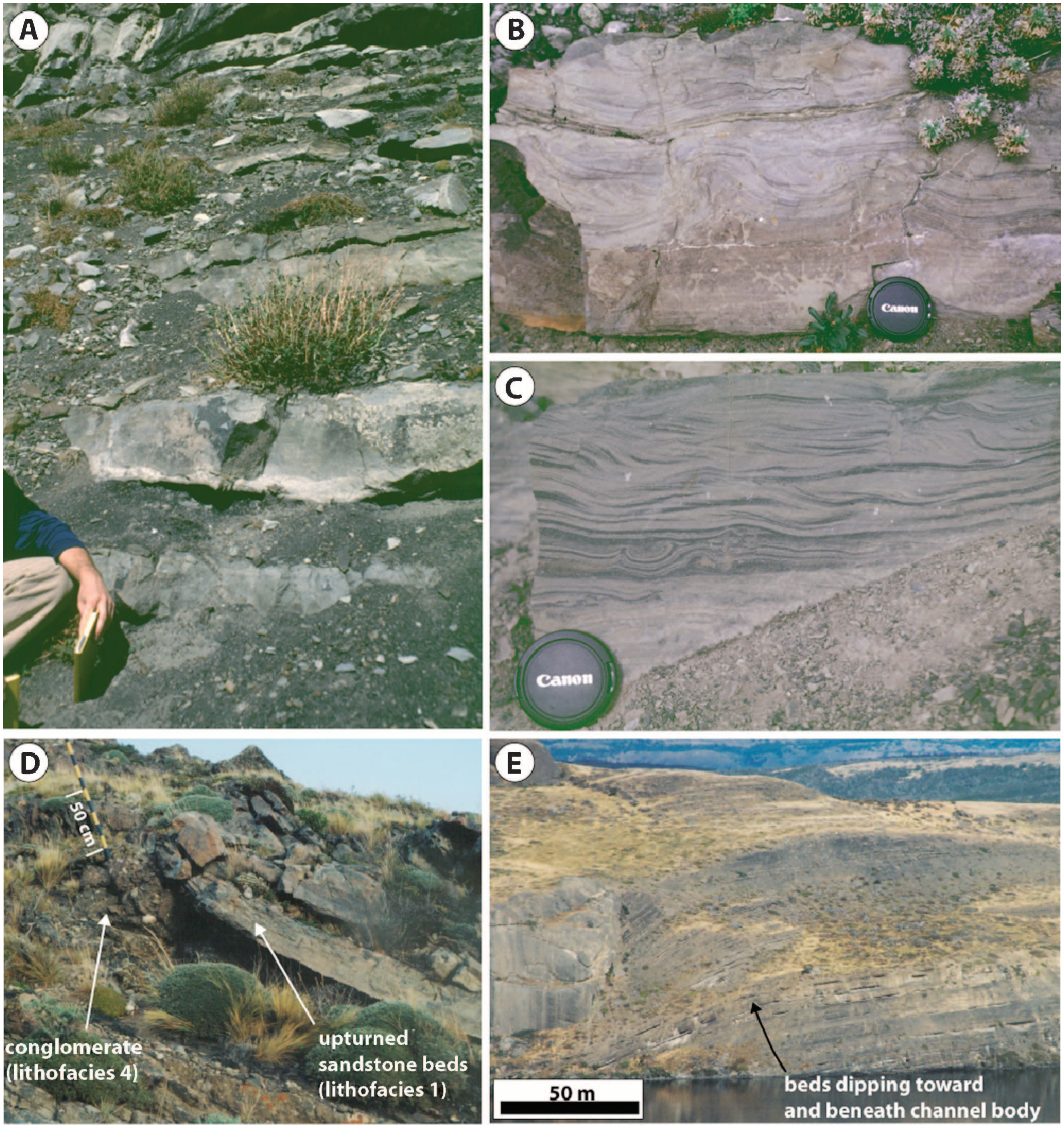

Figure 4. (A) Overview of stratified thin-bedded sandstone and mudstone (lithofacies 1). (B, C) Photographs of sandy gravity-flow deposits (lithofacies 1) characterized by primary sedimentary structures and soft sediment deformation. (D) Upturned sandstone beds adjacent to vertical conglomeratic body (lithofacies 4). (E) Thin-bedded units of lithofacies 1 dipping beneath stratified conglomerate unit (lithofacies 3). This structural deformation results from differential compaction of fine-grained units and coarse-grained, conglomeratic facies.

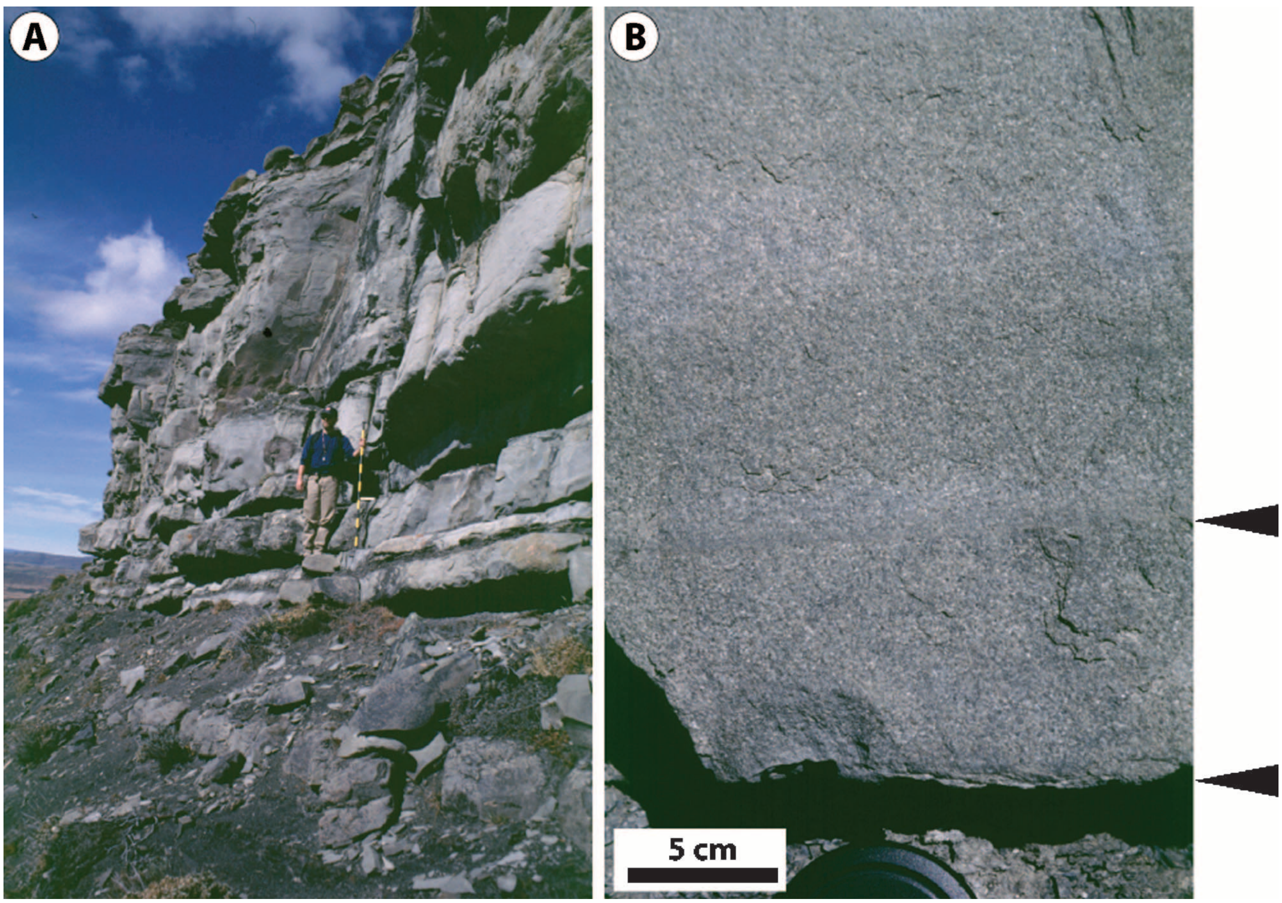

Figure 5. (A) Overview of stratified thick-bedded sandstone (lithofacies 2). (B) Basal part of thick sandstone unit with characteristic upward grain-size coarsening associated with a thin traction carpet. Arrows indicate bed contacts.

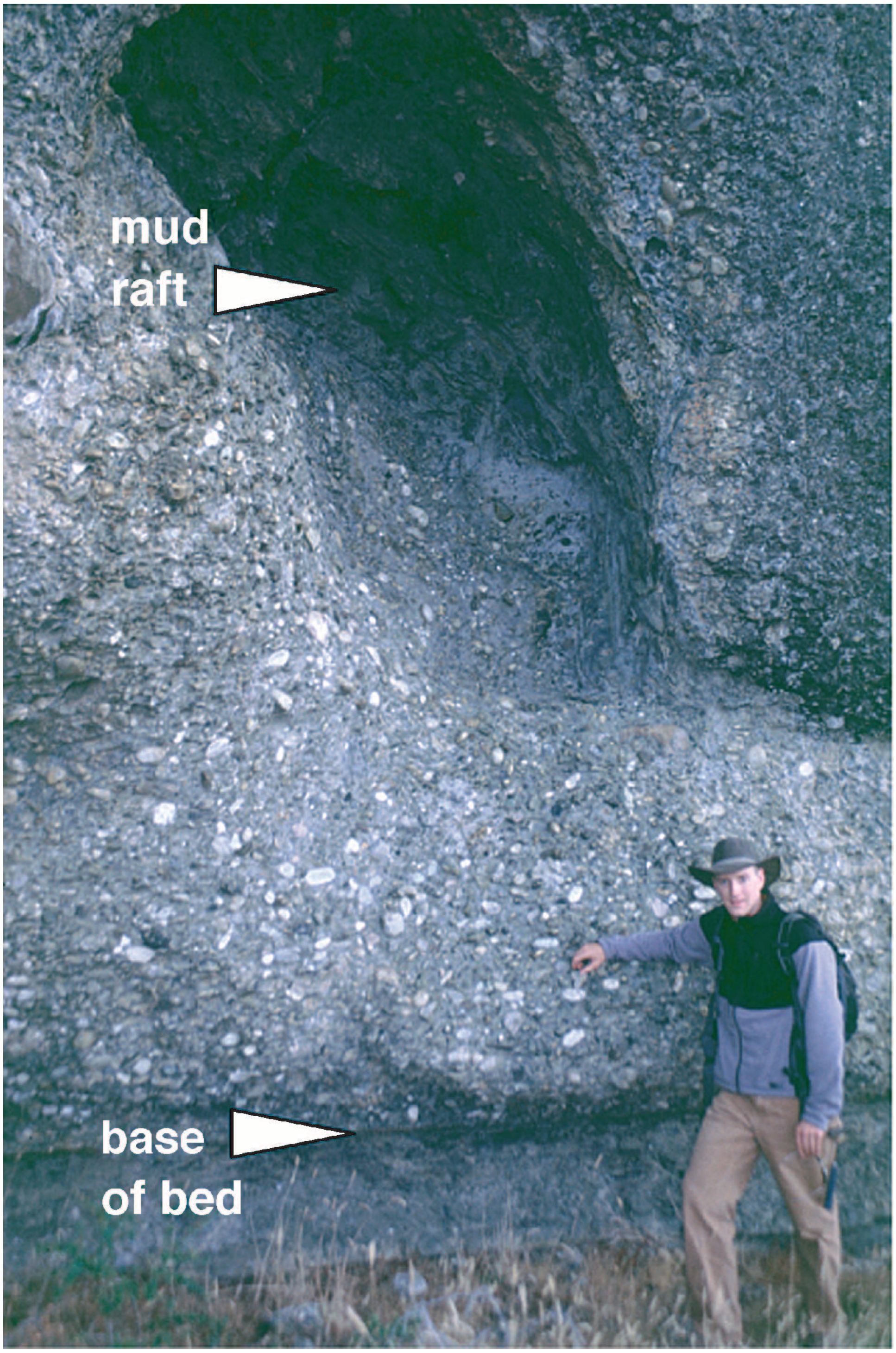

Figure 6. Large mudstone raft block disaggregating into a conglomeratic sedimentation unit and locally increasing matrix mud content (lithofacies 3).

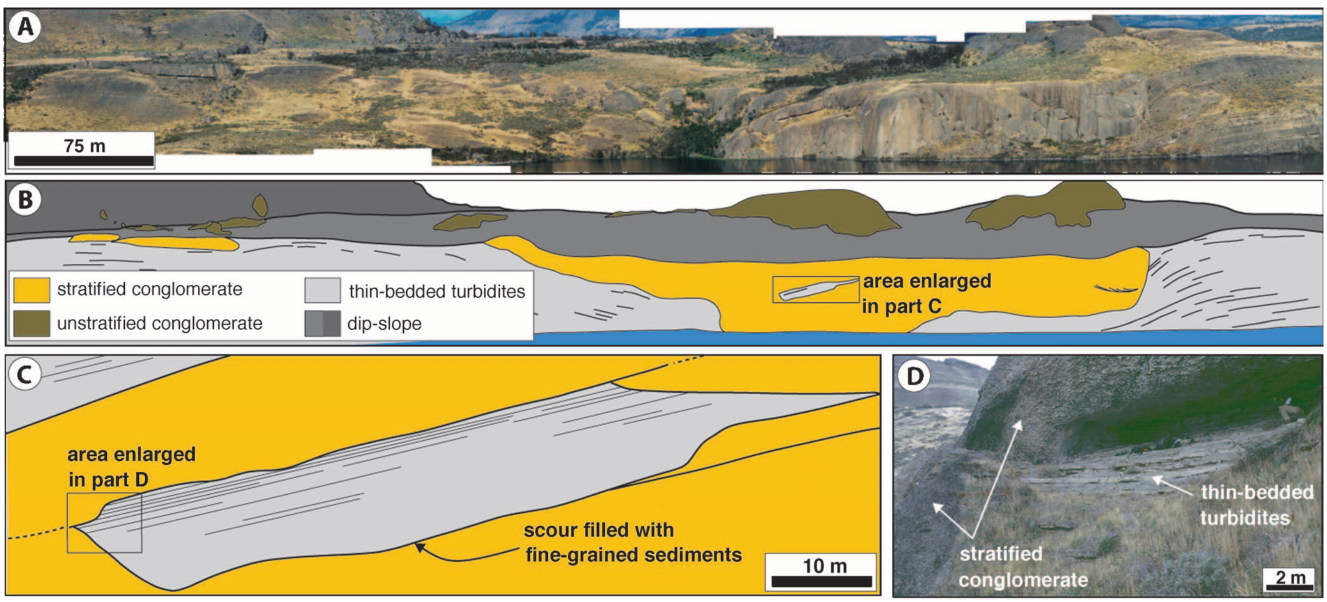

FIGURE 7. (A) Channel-form stratified conglomerate sedimentary bodies on the southern shore of Lago Sofia, with outline of the important features in (B). (C) Large scour feature in the large conglomerate body filled with thin-bedded turbidites. The internal architecture of the conglomerate body is dominated by incisions 2–12 m (6.6–39 ft) deep. (D) Photograph of the incision fill.

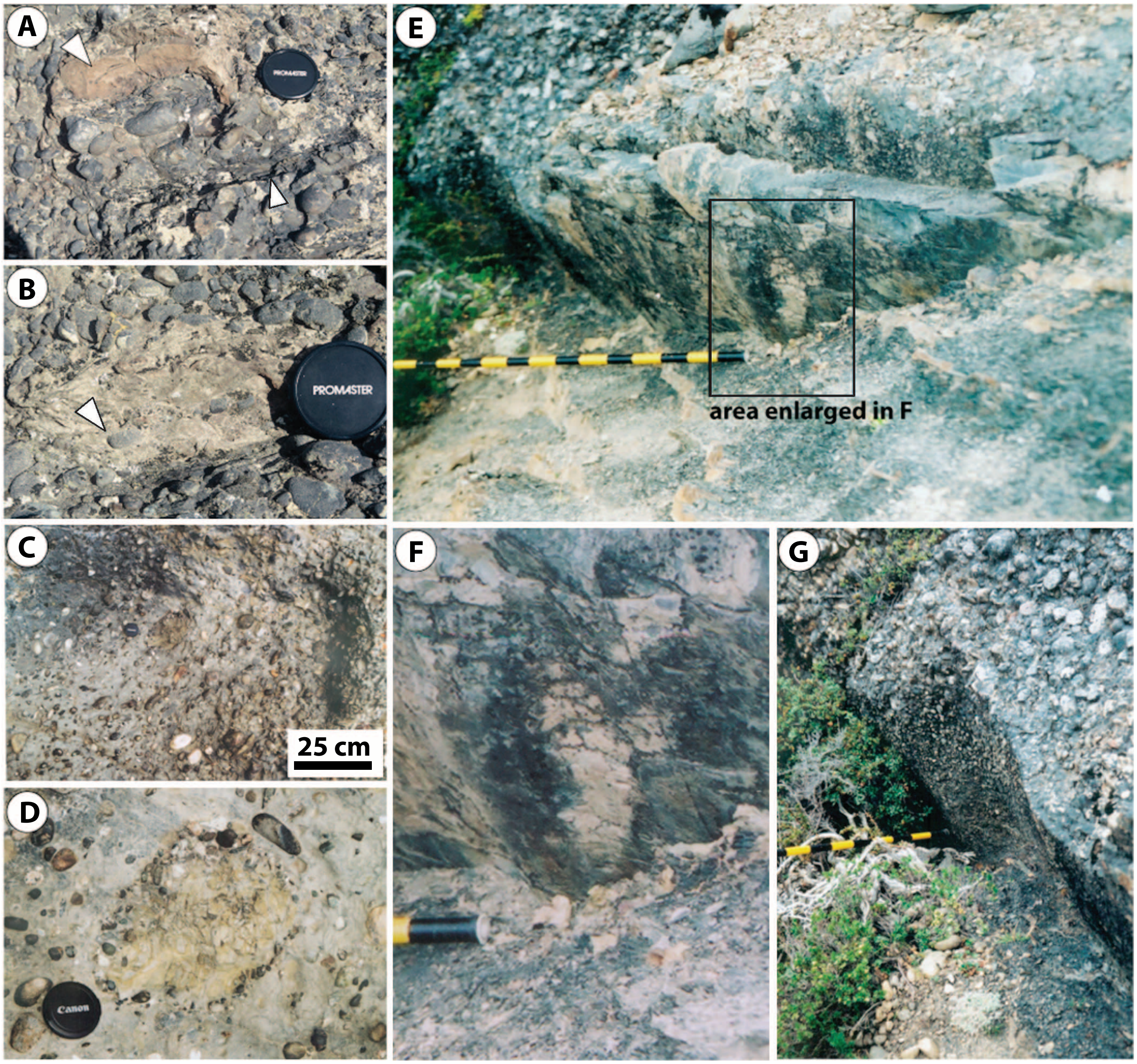

Figure 8. Sedimentary characteristics of injectites. (A, B) Ripped-up turbiditic sandstone and mudstone beds in unstratified conglomerate (lithofacies 4). (C) Muddy matrix-supported conglomerate of lithofacies 4. (D) Armored mud-clast floating in matrix-supported conglomerate. (E) Subvertical sandstone layer at margin of unstratified conglomerate characterized by flutelike grooves. Close-up of groove is presented in (F). (G) Groove on margin of unstratified conglomerate body.

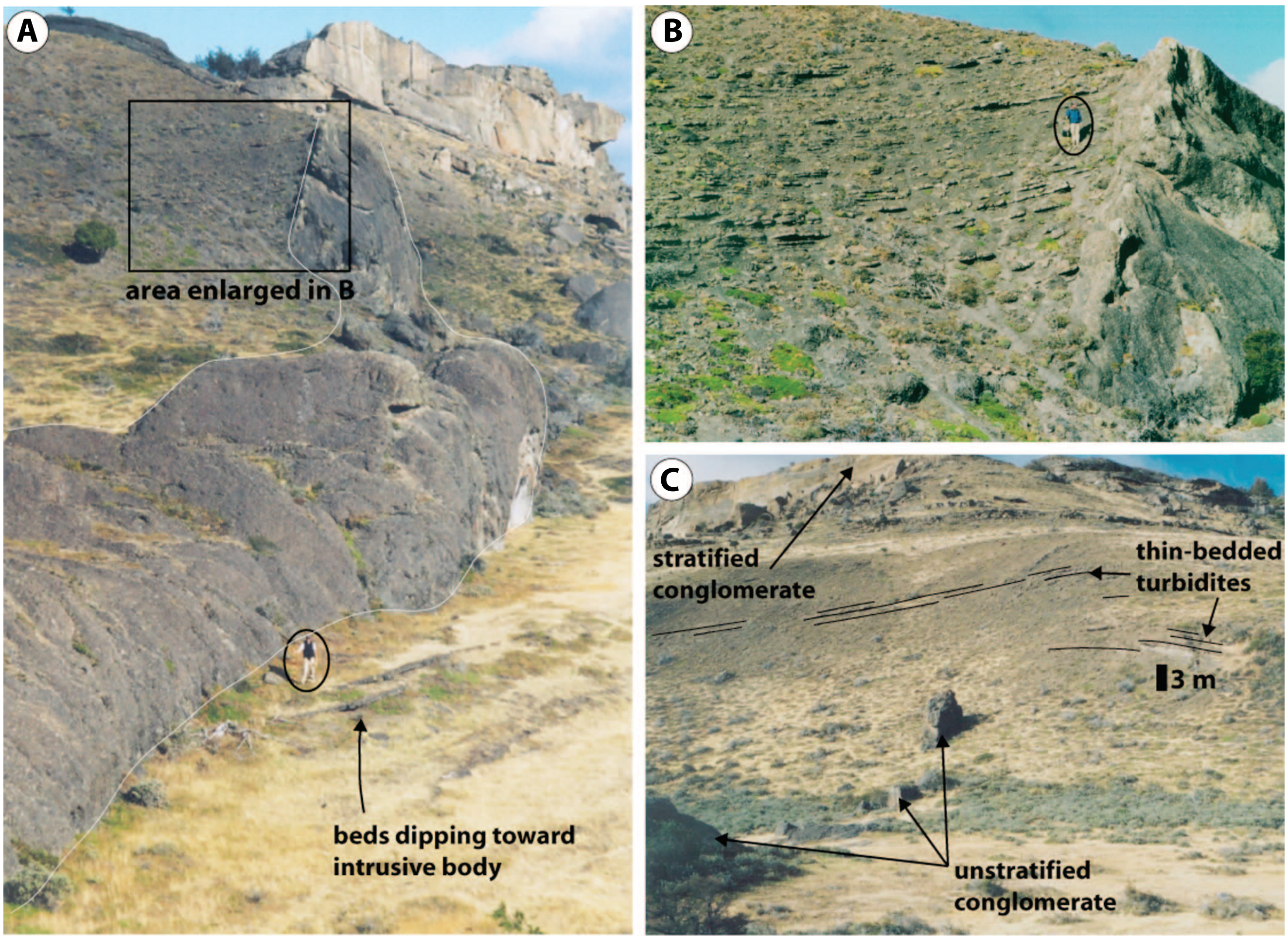

FIGURE 9. (A) Overview of large injectite oriented approximately perpendicular to bedding. (B) Where the injectite thins and is vertical, bedding in the surrounding host rock was bent upward in response to the flow of remobilized sediment. (C) Draping of conglomeratic injectite by thin-bedded turbidites (lithofacies 1) deformed in response to differential compaction.

FIGURE 10. Normally graded injectite. Unstratified conglomerate (lithofacies 4) grades upward into unstratified, poorly sorted sandstone (lithofacies 5).

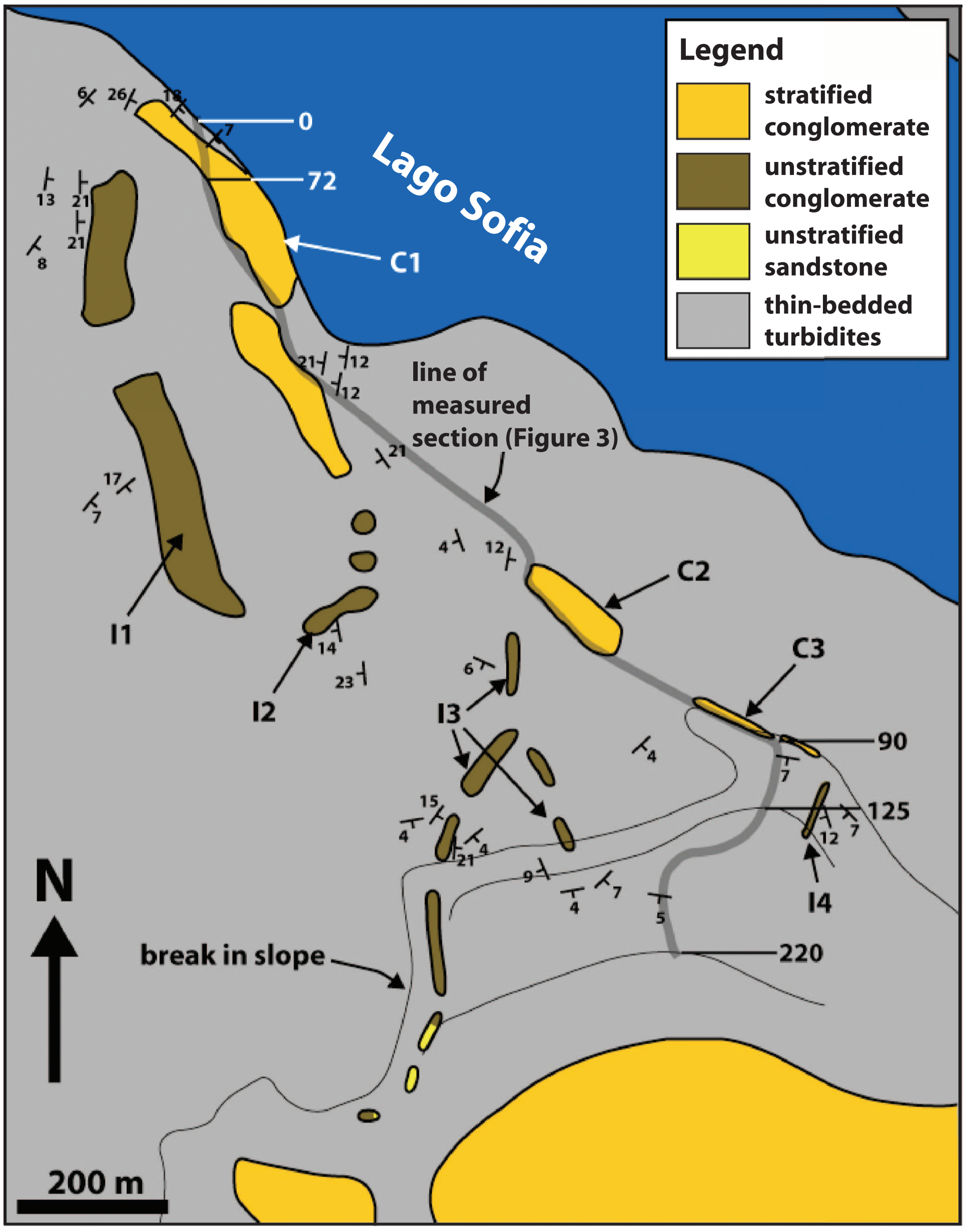

FIGURE 11. Geological map of the study area showing the distribution of various lithofacies, the location of the measured section (detailed in Figure 3), and the orientations of thin turbiditic beds. Channel and injectite bodies discussed in the text are labeled C1–C3 and I1–I4, respectively. The contour lines represent the general topographic relief in the area; detailed maps of the study area are not available.

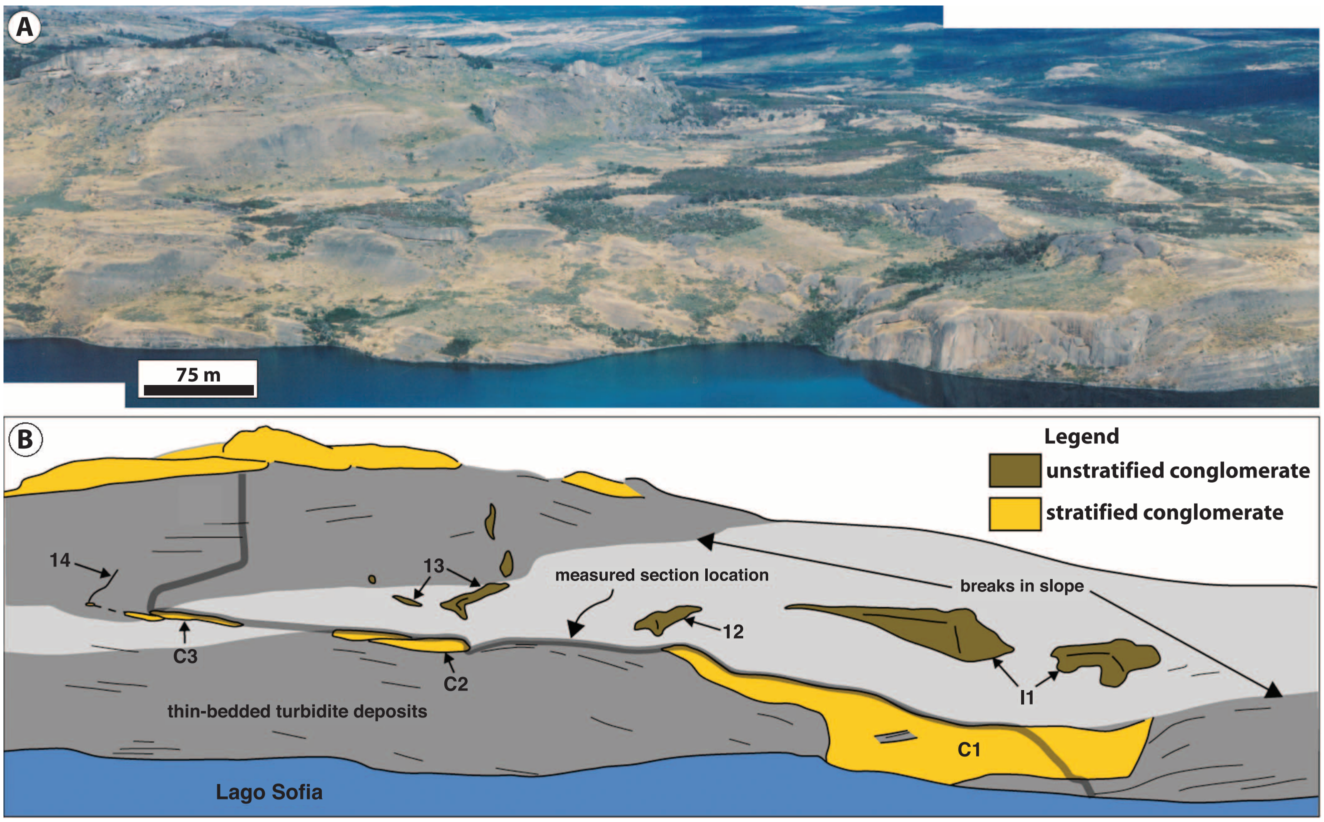

FIGURE 12. (A) Oblique aerial photograph of the entire channel-intrusion complex. (B) Line trace of photograph in (A), showing the distribution of the various facies in the study area. Channel and injectite bodies discussed in the text are labeled C1–C3 and I1–I4, respectively. Note the location of intrusive deposits in close proximity to the margins of the underlying channel bodies.

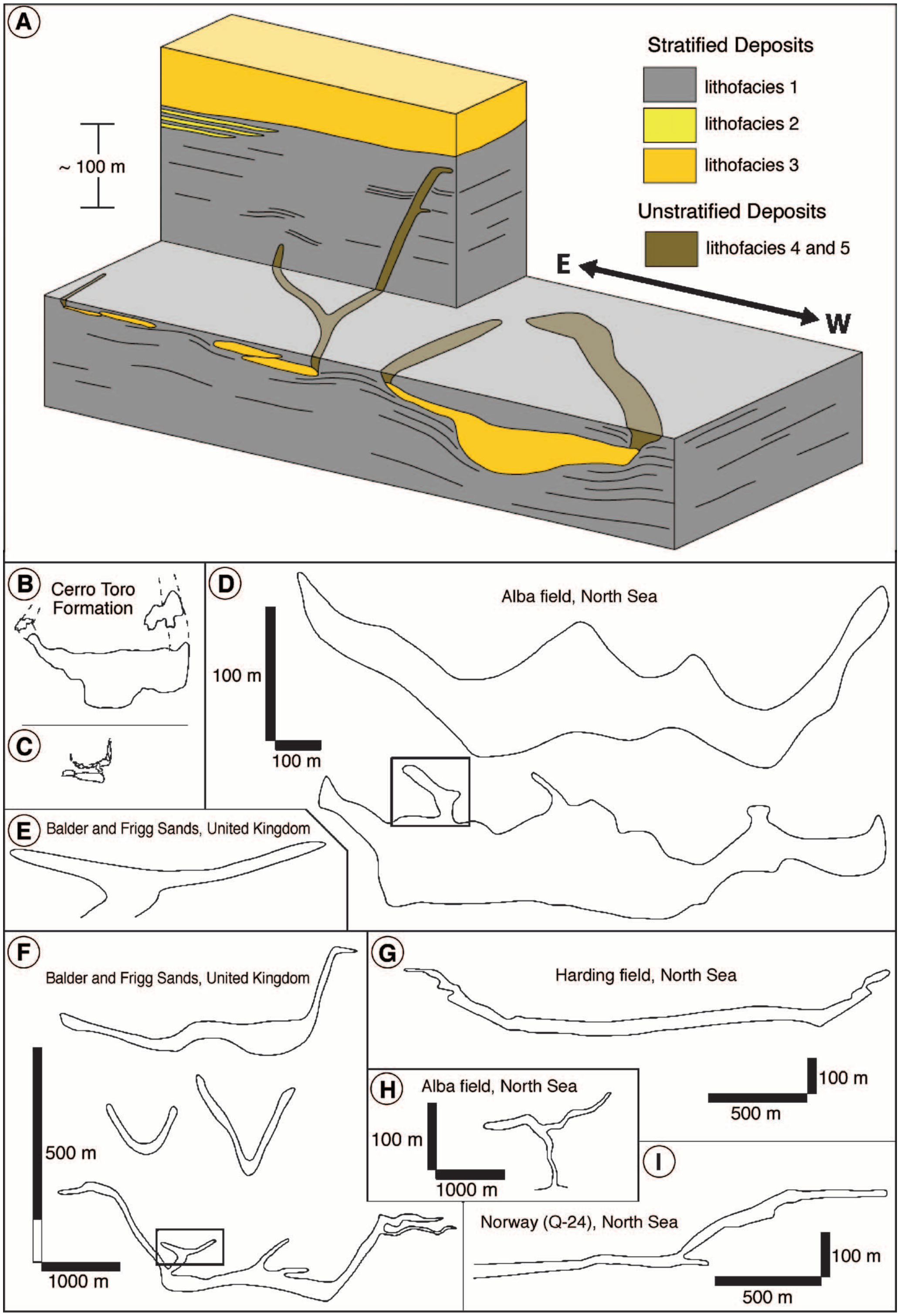

FIGURE 13. Cross sectional geometry and size of various channel deposits and injectite bodies. (A) Generalized 3-D block diagram of stratified deposits and injectites in the Cerro Toro Formation with two-dimensional outlines of channel bodies C1 (B) and C2 (C). (D) Winged channel bodies from the Alba field, United Kingdom. (E) Injectite body in the Balder Formation (United Kingdom) enlarged from the box in (F). Note that all drawings in (B–E) are drawn at the same scale. Box in (D) highlights a relatively small injectite most comparable in scale to the C2 injectite in the Cerro Toro Formation. (F) Variable, large-scale injectite-depositional bodies of the Balder Formation. Winged channel bodies from the United Kingdom (G) and Norwegian (I) sectors of the North Sea. (H) Outline of bifurcating injectite associated with Alba sandstones. Data in (D) to (I) modified from MacLeod et al. (1999), Duranti et al. (2002), Jolly and Lonergan (2002), Hurst et al. (2003a, b), and Huuse et al. (2004).

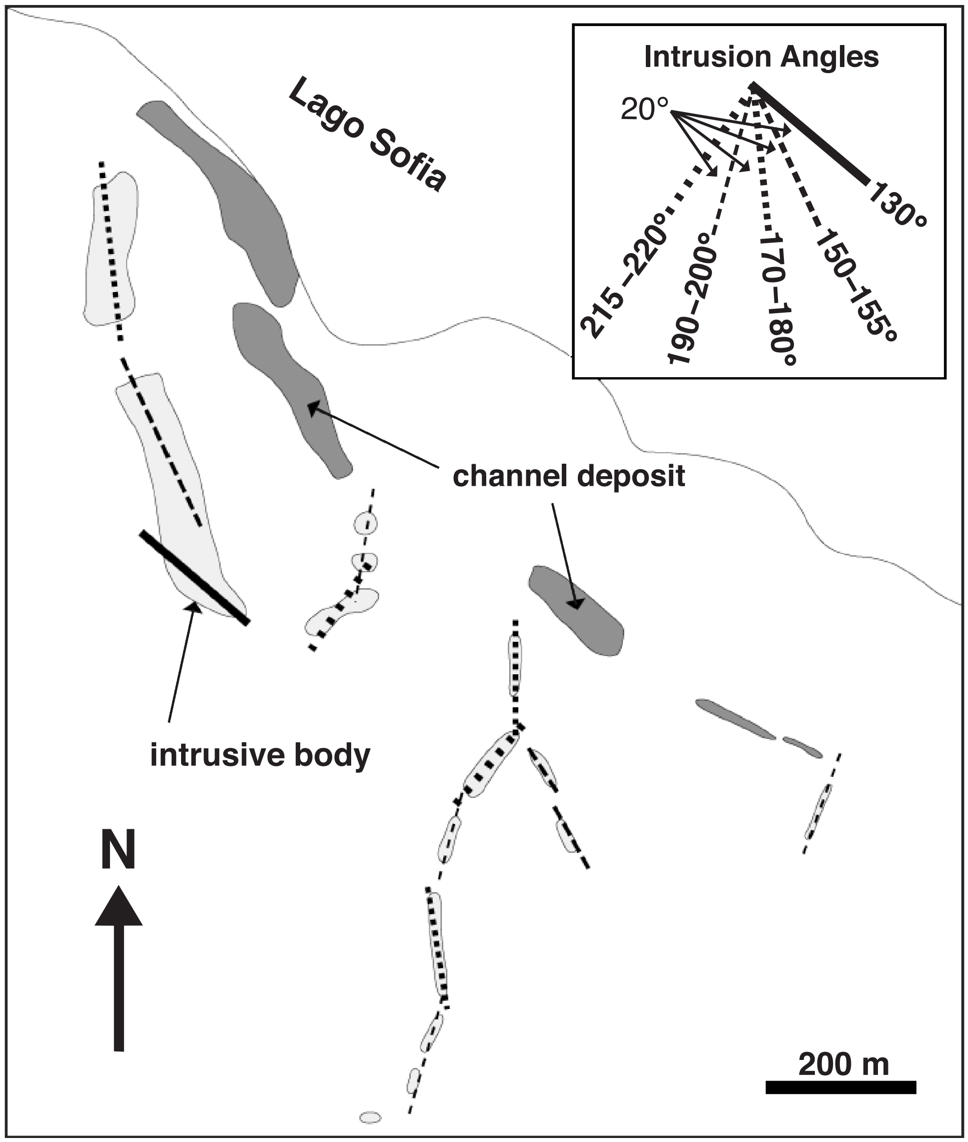

FIGURE 14. Map outlining the orientation of outcropping injectites in the study area. The polygonal arrangement of the injectites suggests that their distribution is structurally controlled. Note that field measurements have not been back rotated, because the regional dip in the area is generally shallow (<10°, Figure 11).